

Hard sphere fluids at surfaces of porous media

Matthias Schmidt

Institut für Theoretische Physik II, Heinrich-Heine-Universität Düsseldorf, Universitätsstraße 1, D-40225 Düsseldorf, Germany

(Received 12 December 2002; published 18 August 2003)

An adsorbate fluid of hard spheres is brought into contact with a semi-infinite porous matrix modeled by immobilized configurations of freely overlapping spheres with a sharp kink one-body density distribution. Comparison of results from a recent density-functional approach to those of our computer simulations yields good agreement for the adsorbate density profile across the matrix surface. We show how the matrix can be replaced by a fictitious external potential that only depends on the distance from the interface, and that leads to the same adsorbate density profile. This potential is found to be a smooth function of distance, due to the geometry of the matrix particles. For high matrix densities, the porous medium becomes practically impenetrable, and its surface behaves like a rough hard wall whose roughness decreases with increasing matrix density.

DOI: 10.1103/PhysRevE.68.021106

PACS number(s): 64.10.+h, 61.20.-p, 61.43.-j, 78.55.Mb

I. INTRODUCTION

Fluids in porous media have considerable technical as well as fundamental importance [1]. Such systems are intrinsically inhomogeneous through the presence of a disordered medium that can be regarded as a random external potential acting on the adsorbed fluid. The behavior of such a confined fluid may be drastically different from that of the same substance in bulk [1,2]. As a theoretical model to study such systems, one often relies on so-called quenched-annealed (QA) fluid mixtures, where the immobilized particles of the quenched species constitute the matrix and the particles of the annealed species represent the adsorbate. Various approaches to such systems exist.

Within the framework of a lattice model the important problem of hysteresis in sorption isotherms was recently considered using a mean-field density-functional approach [3,4]. It was found that hysteresis can occur both with and without an underlying equilibrium phase transition. Subsequently, a pronounced change in the desorption behavior was found if a surface of the matrix is explicitly taken into account [5], and hence, direct contact with the gas reservoir is considered.

For continuum fluids similar inhomogeneous situations have been considered using integral equation theory and computer simulations. Dong, Kierlik, and Rosinberg derived the inhomogeneous replica Ornstein-Zernike equations to treat problems such as the adsorption near a plane boundary of a disordered matrix [6]. Pizio and Sokolowski [7] used a similar approach to investigate an annealed fluid in a slitlike pore filled with quenched hard spheres. They found that the matrix lowers the amount of adsorbed fluid at low chemical potentials and that layering occurs for high chemical potentials. Subsequently, Kovalenko *et al.* [8] extended upon this work and compared results from different integral equation closure relations to those from their computer simulations finding good agreement.

For such inhomogeneous situations density-functional theory (DFT) [9] seems to be a natural tool of investigation. Recently, a DFT, based on Rosenfeld's fundamental-measure theory [10], was proposed that is specially tailored for adsor-

bates in porous media [11]. An explicit approximation for mixtures of particles interacting with either hard core or (vanishing) interactions was given. The particular feature of this QA-DFT approach is that the matrix is described on the level of its one-body density distribution and the free-energy functional is directly the (over all matrix realizations) averaged free energy. This offers great advantages: First, one gains immediate access to matrices that are nonuniform *on average*; second, matrices that are uniform (on average) are described particularly simple, namely, by a *constant* one-body density distribution of quenched particles. This is in contrast to (computationally more involved) approaches that treat the matrix as an external potential [12]. However, the practical usefulness clearly depends on the quality of results. In the original work [11], the structural correlations in (on average) homogeneous matrices were considered and compared to computer simulation results. For both hard sphere and freely overlapping sphere matrices, it was found that the pair correlation functions obtained from the theory are in very good agreement with simulation results. The differing matrix-matrix correlations in these models have an effect on the detailed structure of the adsorbate, and the theory was shown to describe either case well. Subsequently, the problem of phase separation in porous media was treated using a simple model for a colloid-polymer mixture [13]. Besides the practical importance of mesoscopic particles in porous media, this is a convenient model as it displays a (colloid) liquid-vapor phase transition. The DFT results were compared with those from an integral-equation approach based on the replica Ornstein-Zernike relations together with the optimized random phase approximation (ORPA) [13]. All major trends found in the ORPA could be reproduced by the DFT. In particular, it was found that by tuning the matrix-adsorbate interactions either capillary condensation or evaporation is induced. Although these results seem promising, so far the theory has not yet been tested in inhomogeneous situations. This is the aim of the present work.

We use freely overlapping spheres to represent a porous medium and prescribe their density distribution to be a step function as a simple model for the surface of a porous medium. A hard sphere fluid is brought into contact with this model solid, and we obtain its density profile both from the DFT and, as a benchmark, from Monte Carlo computer

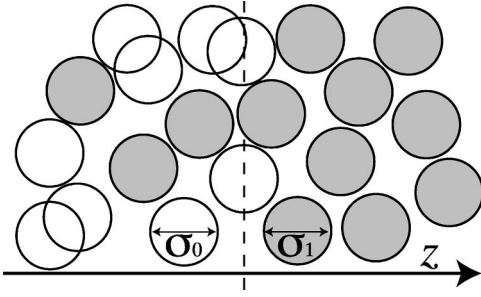


FIG. 1. Model of an adsorbate hard sphere fluid of diameter σ_1 (dark circles) inside a matrix of freely overlapping spheres of diameter σ_0 (white circles). There is hard core interaction between adsorbate and matrix particles. The matrix particles are homogeneously distributed in the half space $z < 0$ generating a planar surface of the porous medium perpendicular to the z direction and located at $z = 0$ (dashed line).

simulations. As expected from the above mentioned bulk results, the plateau density inside the matrix is reproduced well by the theory. Moreover, the interfacial structure is also described very satisfactorily, both on the outside and on the inside of the matrix surface. As a further investigation, we replace the matrix by a fictitious external potential that generates the same adsorbate density profile. This can be naturally done in the DFT framework by requiring the corresponding density profiles to be equal and solving the Euler-Lagrange equation for the fictitious external potential. We find that although the matrix density distribution is a step function, the fictitious external potential is a smoothly varying, slightly oscillating function.

The paper is organized as follows. In Sec. II, we define the model of hard spheres in a matrix of freely overlapping spheres more explicitly. In Sec. III, a brief overview of the theory is given. Section IV is devoted to the simulation method. Results are presented in Sec. V and we conclude in Sec. VI.

II. THE MODEL

We consider an annealed adsorbate of hard spheres (species 1) with diameter σ_1 immersed in a matrix of quenched ideal spheres (species 0) of diameter σ_0 . The interaction between matrix particles and adsorbate particles is again that of hard spheres. Explicitly, there are three pair interactions as a function of the center-to-center distance r between two particles given by

$$V_{00}(r) = 0, \quad (1)$$

$$V_{01}(r) = \begin{cases} \infty & \text{if } r < (\sigma_0 + \sigma_1)/2 \\ 0 & \text{otherwise,} \end{cases} \quad (2)$$

$$V_{11}(r) = \begin{cases} \infty & \text{if } r < \sigma_1 \\ 0 & \text{otherwise,} \end{cases} \quad (3)$$

see Fig. 1 for an illustration of the model. In order to achieve an (on average) inhomogeneous matrix, we consider an external potential acting on the matrix particles given by

$$V_0^{\text{ext}}(z) = \begin{cases} \infty, & z > 0 \\ 0 & \text{otherwise,} \end{cases} \quad (4)$$

where z is the space coordinate perpendicular to the matrix surface. As the matrix alone is a (quenched) ideal gas [Eq. (1)], its density distribution under the influence of Eq. (4) is simply a step function

$$\rho_0(z) = \rho_0^{\text{in}} \Theta(-z), \quad (5)$$

where ρ_0^{in} is the mean density “inside” the matrix and we denote one-body density distribution of species $i=0,1$ by $\rho_i(\mathbf{r})$, where \mathbf{r} is the spatial coordinate.

Packing fractions η_i , $i=0,1$ are used as thermodynamic variables: For the matrix $\eta_0 = \pi \rho_0^{\text{in}} \sigma_0^3 / 6$, where ρ_0^{in} is the number density inside the matrix [see Eq. (5)]. For the adsorbate, we use the overall packing fraction $\eta_1 = \pi \sigma_1^3 N_1 / (6V)$, where N_1 is the number of adsorbate spheres and V is the system volume. In general, the size ratio σ_1 / σ_0 is a further control parameter. We will, however, present results below only for the case of equal sizes, $\sigma_1 = \sigma_1 \equiv \sigma$.

III. THEORY

Let us start with a description of the matrix alone. For general matrix-matrix interactions, the grand potential of the matrix as a functional of its one-body distribution is given as

$$\begin{aligned} \beta \Omega_0[\rho_0] = & \int d\mathbf{r} \rho_0[\ln\{\rho_0(\mathbf{r}) \Lambda_0^3\} - 1] + \beta F_0^{\text{exc}}[\rho_0] \\ & + \beta \int d\mathbf{r} \rho_0(\mathbf{r}) [V_0^{\text{ext}}(\mathbf{r}) - \mu_0], \end{aligned} \quad (6)$$

where $\beta = 1/(k_B T)$, k_B is the Boltzmann constant, T is the absolute temperature, Λ_i is the thermal wavelength, and μ_i is the chemical potential of species i . The first term on the right-hand side of Eq. (6) is the free energy of an ideal gas; the second term is the excess Helmholtz free energy F^{exc} that is due to interparticle interactions. In the present case of vanishing interactions between matrix particles [Eq. (1)], $F_0^{\text{exc}} = 0$. Once $V_0^{\text{ext}}(\mathbf{r})$ is prescribed, the corresponding density profiles is obtained from minimization of the grand functional

$$\frac{\delta \Omega_0[\rho_0]}{\delta \rho_0(\mathbf{r})} = 0. \quad (7)$$

In the present case [Eq. (4)], this is trivial and leads to the above step function for the matrix profile, Eq. (5).

Following Ref. [11] also, the (over all matrix realizations) averaged grand potential of the QA system is expressed as a functional, dependent on both the density distribution of the annealed component and that of the quenched component. Explicitly,

$$\beta\Omega_1[\rho_0;\rho_1]=\int d\mathbf{r}\rho_1(\mathbf{r})[\ln\{\rho_1(\mathbf{r})\Lambda_1^3\}-1]+\beta F_{\text{exc}}[\rho_0;\rho_1] \\ +\beta\int d\mathbf{r}\rho_1(\mathbf{r})[V_1^{\text{ext}}(\mathbf{r})-\mu_1]. \quad (8)$$

Again there is a minimization principle, but, in contrast to the case of a fully annealed binary mixture, this applies only to the adsorbate component

$$\left.\frac{\delta\Omega_1[\rho_0;\rho_1]}{\delta\rho_1(\mathbf{r})}\right|_{\rho_0(\mathbf{r})}=0. \quad (9)$$

The matrix density field $\rho_0(\mathbf{r})$ is treated as a fixed input quantity in Eq. (9). Once the external potential acting on the adsorbate, $V_1^{\text{ext}}(\mathbf{r})$ in Eq. (8), is prescribed, solving Eq. (9) yields the adsorbate one-body density $\rho_1(\mathbf{r})$. This holds for the general case, in the present surface investigation we do not consider such an influence, and hence, restrict ourselves to $V_1^{\text{ext}}(\mathbf{r})=0$.

In general, unknown part in the grand potential, Eq. (8), is the Helmholtz excess free energy functional F_1^{exc} . Here, we rely on the geometrical DFT proposed in Ref. [11]. This is based on both the exact zero-dimensional limit of the QA model under consideration and on Rosenfeld's fundamental measure theory [10]. For technical details, we refer the reader directly to Ref. [11]. To obtain numerical solutions of Eq. (9), we employ a standard iteration procedure [14]. For the special case of constant density fields of both matrix and adsorbate the excess free energy per volume as obtained by applying the density functional to constant density fields is given by

$$\frac{\beta F_{\text{exc}}(\rho_0;\rho_1)}{V} \\ =\frac{3}{\pi\sigma_1^3}\left\{\frac{3\eta_1(\eta_0+s)^3}{e^{2\eta_0}(e^{-\eta_0}-\eta_1)^2s^3}\right. \\ \frac{3\eta_1\eta_0(\eta_0+s)(-2+2\eta_0+s)}{e^{\eta_0}(e^{-\eta_0}-\eta_1)s^3} \\ \frac{\eta_0(2+3(-2+\eta_0)\eta_0)(\eta_0+\ln(e^{-\eta_0}-\eta_1))}{e^{\eta_0}s^3} \\ \left.-\eta_1[3+2\ln(e^{-\eta_0}-\eta_1)]\right\}, \quad (10)$$

where $s=\sigma_0/\sigma_1$.

In order to understand the inhomogeneities caused by the random matrix better, we find it useful to consider an equilibrium pure system under the influence of a fictitious deterministic (nonrandom) external potential V_1^{fict} that possesses the same symmetry as the one-body matrix density distribution; here, $\rho_0(z)$ and hence, $V_1^{\text{fict}}(z)$. The benefit is that $V_1^{\text{fict}}(z)$ is a much simpler function than the external potential corresponding to a given matrix realization that is fully de-

pendent on \mathbf{r} . To relate $V_1^{\text{fict}}(z)$ to the QA system, we impose that the corresponding adsorbate density profiles, $\rho_1(z)$, are the same. In the case of the QA system, this is the average density profile caused by the random medium. In the fictitious potential description, the density profile is the response of the system to $V_1^{\text{fict}}(z)$. Obtaining $V_1^{\text{fict}}(z)$ from $\rho_1(z)$ is straightforward in the DFT, as within this framework the one-to-one correspondence between the external potential and the one-body density distribution is explicit. In the common case, the external potential is known and one solves for the one-body density. Here, the situation is reversed. The one-body density distribution is known [as an output of treating the matrix on the level of its density field, Eq. (9)], and one seeks to obtain the corresponding (fictitious) external potential. Explicitly, the grand potential and minimization condition for this situation are given (upon replacing species index 0 by 1, and setting $V_0^{\text{ext}}=V_1^{\text{fict}}$) through Eqs. (6) and (7), respectively. Solving for the external potential yields (up to an irrelevant additive constant)

$$\beta V_1^{\text{fict}}(\mathbf{r})=-\ln[\rho_1(\mathbf{r})\Lambda_1^3]-\frac{\delta\beta F^{\text{exc}}}{\delta\rho_1(\mathbf{r})}, \quad (11)$$

where the second term on the right-hand side is the one-body direct correlation functional, for which we take Rosenfeld's approximation [10].

IV. COMPUTER SIMULATIONS

In order to assess the accuracy of the theoretical results we have carried out canonical Monte Carlo (MC) computer simulations. The matrix was realized by placing N_0 matrix spheres randomly in one-half of the (cubic and periodic) simulation box. Hence, we consider a periodic system such that Eqs. (4) and (5) describing the matrix distribution are valid within the simulation box $-L/2\leq z < L/2$, where L is the box length. This introduces (as usual) a second matrix surface located at $z=L/2$ (and identified with $z=-L/2$). Strictly speaking, the simulated system is a periodic succession of slit pores and layers of porous material.

The initial configuration for the adsorbate (species 1) is such that all particles are in the empty (of matrix particles) half space. We allow equilibration for half a million MC steps per adsorbate particle and then perform the same number of steps for data production. For each state point considered, we used 30 matrix realizations to perform the average over the disorder. Particle numbers are fixed to $N_0=N_1=512$ and then the system volume $V=L^3$ is adjusted to obtain the prescribed packing fractions. As an illustration, we display a snapshot of a configuration in Fig. 2.

V. RESULTS

For simplicity, we restrict ourselves to cases $\eta_0=2\eta_1$ and $\sigma_0=\sigma_1$. We consider a range of matrix packing fractions $\eta_0=2\eta_1=0.2, 0.3, 0.4$. To obtain theoretical results at these state points, we adjust μ_1 in Eq. (8) to obtain the prescribed η_1 . In Fig. 3, results for the adsorbate density profiles across

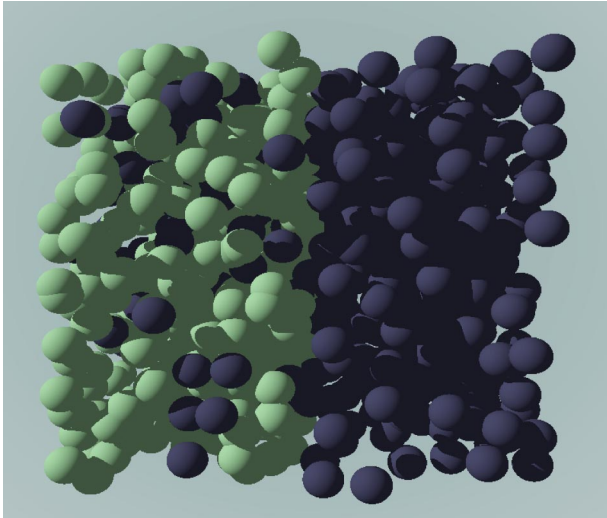


FIG. 2. Snapshot from computer simulation of the hard sphere fluid (dark spheres) adsorbed in a random matrix of freely overlapping spheres (light spheres) of the same size. The matrix particles are distributed homogeneously in the left half of the simulation box and possess packing fraction $\eta_0=0.3$. The overall adsorbate packing fraction is $\eta_1 = \eta_0/2 = 0.15$.

the matrix surface are presented. As mentioned above, we consider a periodic system with periodicity length L . This length is different for the three state points considered, and hence, we display also parts of the periodic images in Fig. 3. These serve also as a guide to assess the actual size of the simulated system.

As the overall packing fraction of the adsorbate η_1 is prescribed, the partitioning between adsorbed fluid inside the matrix and bulk fluid outside the matrix is an output both of the computer simulation and of the theory. For the lowest packing fraction considered, $\eta_0=2\eta_1=0.2$, there is almost

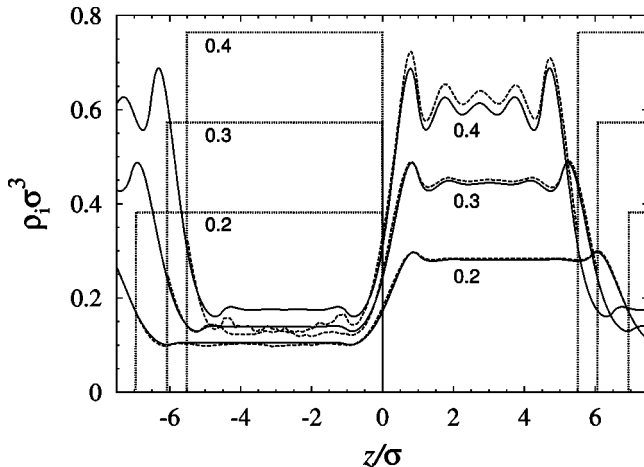


FIG. 3. Density profiles $\rho_1(z)\sigma^3$ of hard spheres at the surface of a porous medium as a function of the (scaled) coordinate z/σ perpendicular to the matrix surface. The matrix density distribution $\rho_0(z)\sigma^3$ is a step function (dotted line) and the system is periodic in the z direction. Results from the DFT (solid lines) and MC simulation (dashed lines) are shown for packing fractions $\eta_0=2\eta_1 = 0.2, 0.3, 0.4$ (as indicated).

perfect agreement between simulation and theoretical results. Both plateau values, inside and outside the matrix, are reproduced very well. Also the smooth crossover at the interface and the damped oscillations outside are reproduced accurately.

Increasing the packing fraction to $\eta_0=2\eta_1=0.3$, both plateau values also increase, hence, the higher density outside presses more adsorbate particles inside. The general agreement is again quite good, however, there are some differences inside the matrix, where the simulation profile is smaller than the theoretical one and displays irregular oscillations (a precursor of this behavior can be already observed for the above case $\eta_0=2\eta_1=0.2$). This behavior may be partially due to insufficient equilibration of the simulation. As we start from a situation where all adsorbate particles are outside the matrix, the MC dynamics needs to migrate the particles inside the matrix. Using simple single moves as we do, this can be a slow process at high matrix densities. This effect then may lead to a slightly higher density outside the matrix than that in true equilibrium. Moreover, in general, the matrix can have cavities that are kinetically inaccessible by the MC dynamics. As the DF is grand-canonical it will fill such cavities by coupling to the particle reservoir. This constitutes a principle difference between both approaches. For $\eta_0=2\eta_1=0.4$, the discrepancy grows worse, but still the agreement is reasonable. Here, pronounced oscillations develop outside, and the situation is more that of a slit pore than that of decoupled surfaces. Also inside the matrix some layering is predicted by the theory, which can, however, only be guessed from the simulation data.

That the theory works well outside the matrix is to be expected, as our theory reduces in the absence of matrix particles to the very accurate Rosenfeld hard sphere functional. However, in the present case the inhomogeneity is caused by the matrix surface and that this is described so accurately can be rated as a success of the current approach.

We display results for the fictitious external potential in Fig. 4. Normalization is such that $V_1^{\text{fict}}(z)=0$ outside the matrix (i.e., $z=3\sigma$). The plateau value inside the matrix (i.e., $z=-3\sigma$), when reinterpreted in the binary QA system, is the chemical potential change required to move a particle from outside to inside. In the binary model, this is solely due to a reduction of entropy for the particle in the confining matrix. In contrast to the sharp kink matrix density profile $V_1^{\text{fict}}(z)$ has a smooth, slowly varying shape. Considering the interface located at $z=0$, one observes deviations from the plateau values inside and outside the matrix in the range of about $-\sigma < z < \sigma$, consistent with a geometrical picture of the surface.

As the density is increased not only the vertical scale of $V_1^{\text{fict}}(z)$ changes, but also its shape. To demonstrate this, we show in Fig. 4 the result for $\eta_0=2\eta_1=0.2$, but multiplied by a factor of 2.78 to get agreement of the potential strength inside the matrix for the case $\eta_0=2\eta_1=0.4$. It can be clearly seen that the actual $V_1^{\text{fict}}(z)$ is a steeper function than would be expected from the simple rescaling. However, these differences are still small taking into account the considerable change in densities. In principle, this opens possi-

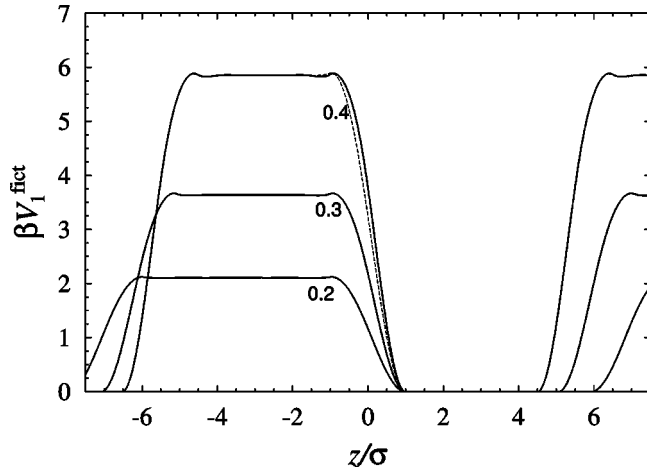


FIG. 4. Fictitious external potentials $\beta V_1^{\text{fict}}(z)$ as a function of the (scaled) coordinate z/σ for the same state points as in Fig. 3. $V_1^{\text{fict}}(z)$ is constructed to generate the same adsorbate density distribution $\rho_1(z)$ as the inhomogeneous porous matrix with density field $\rho_0(z)$ (see Fig. 3). The dashed line is the result for $\eta_0 = 2\eta_1 = 0.2$, but multiplied by a factor of 2.78; compare with the case $\eta_0 = 2\eta_1 = 0.4$.

bilities to a simplified description of such systems.

To conclude this section, we present theoretical results for two further paths along varying density. We will consider a single surface (without periodic images). To control the adsorbate, we prescribe its packing fraction in the half space without matrix, $\eta_1 = (\pi\sigma_1^3/6)\rho_1(z \rightarrow \infty)$. Practically, this acts as an adsorbate reservoir that is in direct contact with the porous medium. As a first case, we fix the matrix density at the highest packing fraction considered above, $\eta_0 = 0.4$, and increase the bulk packing fraction outside over a range $\eta_1 = 0.1, 0.2, 0.3, 0.4$, see Fig. 5 for results. Increasing the density outside increases the plateau density inside the matrix monotonically. For $\eta_1 = 0.1$, the profile is very smooth across the surface. Upon increasing η_1 pronounced oscillations outside develop and also somewhat smaller (in amplitude) oscillations are apparent for $z < 0$. The wavelength is of the order of the particle size, hence, as expected, these oscillations are due to packing effects of the particles. Figure 5 also shows results for the fictitious external potential. It is remarkable that the plateau value inside the matrix increases as a function of the *adsorbate* density. Hence, an adsorbate fluid at a higher density experiences a higher energy penalty, although the matrix density is unchanged.

The second path that we investigate is at constant bulk density outside, $\eta_1 = 0.4$, and increasing $\eta_0 = 0.1, 0.2, 0.4, 0.8, 1.5, 3$, see Fig. 6. For small matrix density, $\eta_0 = 0.1$, the adsorbate density remains almost constant, only a slight decrease is observed for $z < 0$. Increasing η_0 lowers ρ_1 inside the matrix considerably. For $\eta_0 = 1$, it is vanishing on the scale of the plot. Note that as the matrix consists of freely overlapping spheres, $\eta_1 = 1$ does not correspond to space filling, rather there remain occasional free voids inside the matrix. The surface of the matrix at such high densities is hardly penetrable and practically constitutes a rough hard wall with a random surface structure. Increasing further to

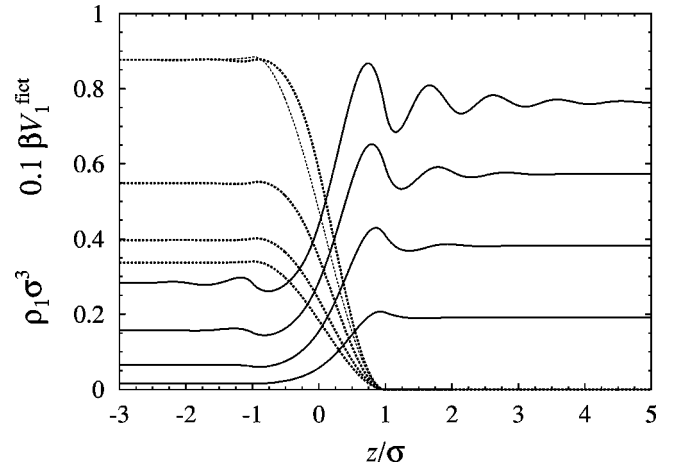


FIG. 5. Adsorbate density profiles $\rho_1(z)\sigma^3$ (solid lines) and fictitious external potentials $\beta V_1^{\text{fict}}(z)$ (dotted lines, scaled by a factor of 0.1) as a function of the distance from the matrix surface z/σ for matrix packing fraction $\eta_0 = 0.4$ and different reservoir adsorbate packing fractions $\eta_1 = 0.1, 0.2, 0.3, 0.4$ (from bottom to top). The matrix particles are homogeneously distributed in the half space $z < 0$. The fictitious external potentials generate the same $\rho_1(z)$ in a pure hard sphere fluid as the porous matrix. The thin dotted line is the fictitious external potential for $\eta_1 = 0.1$, but multiplied by a factor of 2.6; compare with the case $\eta_1 = 0.4$.

$\eta_0 = 3$ leads to more compact roughness. In the limit $\eta_0 \rightarrow \infty$, the matrix becomes a *smooth* hard wall located at $z = \sigma/2$. In Fig. 6, the density profile at a hard smooth wall is shown, and one can verify, from the structure of the DFT, that this is indeed the correct asymptotic behavior. As an illustration, we show in Fig. 7 views in the direction perpendicular towards the matrix surface. The matrices shown in Figs. 7(a,b) possess packing fractions $\eta_0 = 1, 3$, respectively, corresponding to the two densest matrices where results are shown in Fig. 6. It is clear that even in the case $\eta_0 = 3$, there

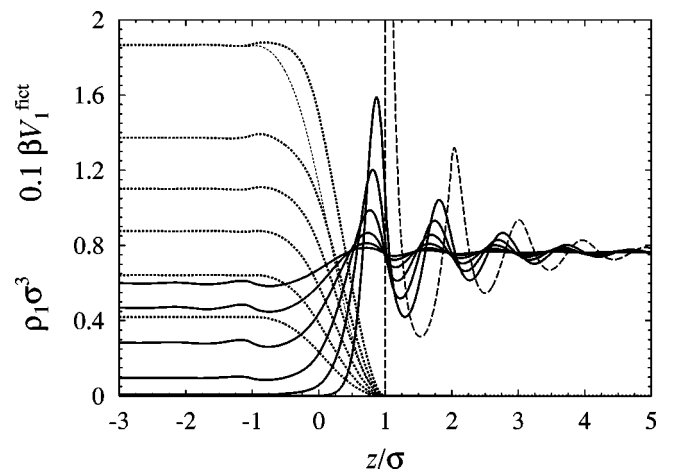


FIG. 6. Same as Fig. 5, but for fixed reservoir packing fraction $\eta_1 = 0.4$ and different matrix packing fractions $\eta_0 = 0.1, 0.2, 0.4, 0.8, 1.5, 3$ (from bottom to top). The dashed line indicates the hard wall result for $\rho_1(z)$; this is approached as $\eta_0 \rightarrow \infty$. The thin dotted line is the fictitious external potential for $\eta_0 = 0.2$, but multiplied by a factor of 2.9; compare with the case $\eta_0 = 3$.

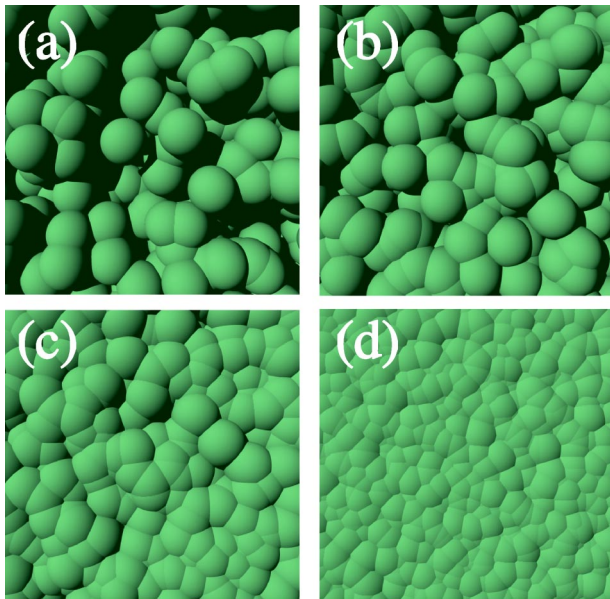


FIG. 7. Surface structure of randomly overlapping spheres with packing fractions $\eta_0=1$ (a), $\eta_0=3$ (b), $\eta_0=10$ (c), $\eta_0=100$ (d).

are considerable voids in the surface. The matrix packing fraction needs to be increased further in order to level out these voids, see Figs. 7(c,d) for $\eta=10,100$, respectively. Even for $\eta_0=100$, there remains residual surface roughness, although clearly the smooth wall is almost obtained.

VI. CONCLUSIONS

In conclusion, we have considered the behavior of an adsorbate hard sphere fluid at the surface of a porous matrix. The matrix is modeled by freely overlapping spheres with a

step function density distribution that models the surface (towards an adsorbate reservoir) of a porous medium. We have applied for the first time a recent DFT approach to such an inhomogeneous situation and have performed computer simulations in order to provide benchmark results. The theoretical results for the adsorbate one-body density distribution across the matrix interface are found to be in good agreement with simulation results up to considerably high matrix packing fractions, i.e., low porosities. The benefit of the theoretical approach is that the required double average over the equilibrated fluid configurations and the quenched disorder is already taken [11]; no subsequent averaging “by hand” is necessary. Within the DFT framework, we relate the QA model to a pure system exposed to a fictitious external potential that only depends on the perpendicular distance from the interface. Although the matrix surface has a sharp kink shape, the fictitious potential is found to be a smooth function that crosses over from its plateau values inside and outside the matrix over about two sphere diameters.

As an outlook to possible future work, we mention the possibility of a further explicit external potential, such as a gravitational field or confinement by walls. Furthermore, as we have shown, the important problem of surface roughness can be treated. Also the behavior for more asymmetric sizes and hence, the effect of size selectivity in porous media is an interesting topic.

ACKNOWLEDGMENTS

Very useful discussions with M.-L. Rosinberg, G. Tarjus, G. Kahl, R. Evans, H. Löwen, and P. Wessels are gratefully acknowledged. A. R. Denton is thanked for providing computer time at NDSU and P. Wessels is thanked for a critical reading of the manuscript. This work was supported by the DFG within the SFB TR6.

-
- [1] L.D. Gelb, K.E. Gubbins, R. Radhakrishnan, and M. Sliwinski-Bartkowiak, Rep. Prog. Phys. **62**, 1573 (1999).
 - [2] R. Evans, J. Phys.: Condens. Matter **2**, 8989 (1990).
 - [3] E. Kierlik, P.A. Monson, M.L. Rosinberg, L. Sarkisov, and G. Tarjus, Phys. Rev. Lett. **87**, 055701 (2001).
 - [4] E. Kierlik, P.A. Monson, M.L. Rosinberg, and G. Tarjus, J. Phys.: Condens. Matter **14**, 9295 (2002).
 - [5] M.L. Rosinberg, E. Kierlik, and G. Tarjus, Europhys. Lett. **62**, 377 (2003).
 - [6] W. Dong, E. Kierlik, and M.L. Rosinberg, Phys. Rev. E **50**, 4750 (1994).
 - [7] O. Pizio and S. Sokolowski, Phys. Rev. E **56**, R63 (1997).
 - [8] A. Kovalenko, S. Sokolowski, D. Henderson, and O. Pizio, Phys. Rev. E **57**, 1824 (1998).
 - [9] R. Evans, in *Fundamentals of Inhomogeneous Fluids*, edited by D. Henderson (Dekker, New York, 1992), p. 85.
 - [10] Y. Rosenfeld, Phys. Rev. Lett. **63**, 980 (1989).
 - [11] M. Schmidt, Phys. Rev. E **66**, 041108 (2002).
 - [12] L.J. Frink, A.G. Salinger, M.P. Sears, J.D. Weinhold, and A.L. Frischknecht, J. Phys.: Condens. Matter **14**, 12 167 (2002).
 - [13] M. Schmidt, E. Schöll-Paschinger, J. Köfinger, and G. Kahl, J. Phys.: Condens. Matter **14**, 12 099 (2002).
 - [14] The tensorial weight functions of Ref. [11] [see also P. Tarazona, Phys. Rev. Lett. **84**, 694 (2000)] are neglected in the numerical treatment. This is a good approximation in the present planar symmetry.